Chemical Research in Toxicology

Article

Cite This: Chem. Res. Toxicol. 2018, 31, 291−301

pubs.acs.org/crt

Activation of TRPV3 by Wood Smoke Particles and Roles in Pneumotoxicity

Cassandra E. Deering-Rice,[†] Nam Nguyen,[†] Zhenyu Lu,[†] James E. Cox,[‡] Darien Shapiro,[†] Erin G. Romero,[†] Virginia K. Mitchell,[†] Katherine L. Burrell,[†] John M. Veranth,[†] and Christopher A. Reilly*[,†]

[†]Department of Pharmacology and Toxicology, Center for Human Toxicology, University of Utah, 30 South 2000 East, Room 201 Skaggs Hall, Salt Lake City, Utah 84112, United States

[‡]Department of Biochemistry, Emma Eccles Jones Medical Research Building, University of Utah, Room A306, 15 North Medical Drive East, Salt Lake City, Utah 84112, United States

Supporting Information

ABSTRACT: Wood/biomass smoke particulate materials (WBSPM) are pneumotoxic, but the mechanisms by which these materials affect lung cells are not fully understood. We previously identified transient receptor potential (TRP) ankyrin-1 as a sensor for electrophiles in WBSPM and hypothesized that other TRP channels expressed by lung cells might also be activated by WBSPM, contributing to pneumotoxicity. Screening TRP channel activation by WBSPM using calcium flux assays revealed TRPV3 activation by materials obtained from burning multiple types of wood under fixed conditions. TRPV3 activation by WBSPM was dependent on the chemical composition, and the pattern of activation and chemical components of PM agonists was different from that of TRPA1. Chemical analysis of particle constituents by gas chromatography−mass spectrometry and principal component analysis indicated enrichment of cresol, ethylphenol, and xylenol analogues, plus several other chemicals among the most potent samples. 2,3-, 2,4-, 2,5-, 2,6-, 3,4-, and 3,5-xylenol, 2-, 3-, and 4-ethylphenol, 2-methoxy-4-methylphenol, and 5,8-dihydronaphthol were TRPV3 agonists exhibiting preferential activation versus TRPA1, M8, V1, and V4. The concentration of 2,3- and 3,4-xylenol in the most potent samples of pine and mesquite smoke PM (<3 μm) was 0.1−0.3% by weight, while that of 5,8-dihydronaphthol was 0.03%. TRPV3 was expressed by several human lung epithelial cell lines, and both pine PM and pure chemical TRPV3 agonists found in WBSPM were more toxic to TRPV3-over-expressing cells via TRPV3 activation. Finally, mice treated sub-acutely with pine particles exhibited an increase in sensitivity to inhaled methacholine involving TRPV3. In summary, TRPV3 is activated by specific chemicals in WBSPM, potentially contributing to the pneumotoxic properties of certain WBSPM.

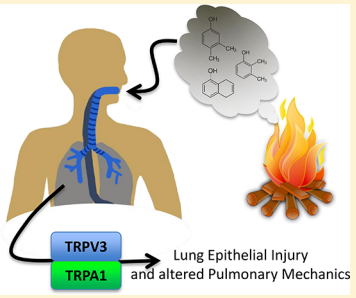

INTRODUCTION

Wood and biomass smoke emissions are frequent indoor and outdoor air pollutants and a major public health concern.[1,2] Wood/biomass smoke particulate materials (WBSPM) form by condensation of semi-volatile chemicals in smoke plumes and are chemically distinct from many other forms of environmental PM. However, mechanisms by which WBSPM affect the lungs and human health are not fully understood.

Wood and biomass particles are pneumotoxic. Episodic exposures for humans (typically in the range of 0.1−1 mg/m^3 for a few hours to days) can result from nearby forest and range fires, crop burning, and the occasional use of wood stoves and fireplaces in homes. Chronic exposures occur frequently in under-developed locations where biomass is burned for heat and in open, poorly ventilated, inefficient cook stoves. Billions of people are exposed to WBSPM as a result of their reliance on wood/biomass as a primary fuel source, with exposures often reaching levels as high as 8−9 mg/m^3 for multiple hours per day, for multiple years.[1,2]

Pulmonary irritation, altered pulmonary immune functions, exacerbation of asthma and cardiovascular diseases, increased rates of respiratory infections, and increased risks for developing chronic obstructive pulmonary disease (COPD)/emphysema have been linked to WBSPM exposure.[3−8] For example, WBSPM (PM_{10} typically exceeding 0.15−0.2 mg/m^3) has been correlated with increased rates of hospital visits for respiratory complications, including the exacerbation of asthma and COPD.[9−18] A formative study in which wood stoves in homes in Libby, MT, USA, were replaced with low-emission wood stoves reported ∼30% lower ambient $PM_{2.5}$ attributed to reduced WBSPM emissions, which correlated with a 20−60% reduction in respiratory infections and other health-related end points among children.[19] Finally, meta-analysis studies estimate a ∼2-fold greater risk for developing COPD associated with WBSPM exposure[20−23] and odds ratios of 1.5−2.3 associated with living in households using biomass fuels for cooking, versus cleaner fuels.[24,25]

Oxidants, reactive oxygen species, and other reactive chemicals are known to contribute to the acute pro-inflammatory and

Received: December 18, 2017
Published: April 16, 2018

DOI: 10.1021/acs.chemrestox.7b00336
Chem. Res. Toxicol. 2018, 31, 291−301

cytotoxic effects of WBSPM.[26−29] We previously characterized the activation of the electrophile/oxidant-sensitive transient receptor potential ankyrin-1 (TRPA1) ion channel in cultured mouse trigeminal neurons and A549 cells by electrophiles and resin acids found in pine and mesquite PM.[30] TRPA1 activation in C-fiber neurons is a mechanism by which WBSPM likely irritates the airways and promotes cough and neurogenic inflammation/edema.

Unlike in A549 cells, TRPA1 is typically expressed at low/non-detectable levels in normal human lung epithelial cells. However, these cells are also impacted in specific ways by WBSPM. In A549 cells, we reported that the TRPA1 antagonist HC-030031 failed to fully inhibit Ca^{2+} flux caused by pine PM.[30] In preliminary studies we also found that primary human lung epithelial cells lacking TRPA1 mRNA expression and Ca^{2+} flux in response to prototypical TRPA1 agonists exhibited Ca^{2+} flux following wood smoke PM treatment that was not affected by a TRPA1 antagonist. Combined, these data suggested the existence of additional wood smoke-sensitive Ca^{2+} channels in lung epithelial cells, which may be relevant to the toxic effects of WBSPM on these cells. Here, we report activation of TRPV3 by specific chemicals present in selected wood smoke PM, TRPV3 expression by multiple human lung epithelial lines, and a role for TRPV3 in WBSPM cytotoxicity *in vitro* and airway hypersensitivity in mice.

EXPERIMENTAL PROCEDURES

Chemicals. Chemicals were purchased from Sigma-Aldrich (St. Louis, MO) or Thermo-Fisher Scientific (Waltham, MA) unless otherwise specified. The TRPV3 antagonist 2-(5-trifluoromethyl-pyridine-2-ylsulfanyl)-1-(8-methyl-3,4-dihydro-2*H*-quinolin-1-yl)-ethanone (TRPV3 antagonist) was synthesized as previously described.[31]

Wood Smoke Particles. Size-fractionated wood smoke PM was produced as previously described.[30] Approximately 10 g portions of fresh, wet, aged, or dry Austrian pine, mesquite chips, and scrub oak collected from the foothills of Salt Lake Valley were burned in a laboratory furnace, and the PM was collected using an Anderson cascade impactor. Depending upon the fuel source, the yield of PM was 0.2−2%.

Diesel Exhaust Particles (DEPs). DEPs were from three sources: the tailpipe of an on-road "black smoker" 2004 Ford F350 truck (Black Smoker), heavy truck diesel particle filter regeneration/cleaning (Filter DEP), and NIST (SRM2975). DEPs were either suspended in treatment solutions as described below or extracted with ethanol to produce an oily, tar-like material previously shown to be enriched in TRPA1 agonists, and similar in consistency to the wood smoke PM used in this study.[30,32]

Preparation of Wood Smoke Particle/Diesel Exhaust Particle Extract Treatment Solutions. Each material/residue was re-suspended in DMSO to an initial concentration of 230 mg/mL and subsequently diluted to the final working concentrations in cell culture media. For cell treatments, the final concentration of DMSO in the treatment solutions was ≤1% (v/v). For screening TRP channel activation, concentrations of 0, 0.58, 1.15, and 2.3 mg/mL extract (equivalent to 0, 45, 90, and 180 $\mu g/cm^2$) were used.

Cells. Cells were maintained in a humidified cell culture incubator at 37 °C with a 95% air:5% CO_2 atmosphere. HEK-293 cells (ATCC; Rockville, MD) were cultured in DMEM:F12 media containing 5% fetal bovine serum and 1x penicillin/streptomycin. Human TRP channel over-expressing HEK-293 cells were generated as previously described[33,34] and were cultured in DMEM:F12 media containing 5% fetal bovine serum, 1x penicillin/streptomycin, and Geneticin (300 $\mu g/mL$). Human adenocarcinoma (A549) cells (ATCC; Rockville, MD) were cultured in DMEM containing 5% FBS and 1x penicillin/streptomycin. BEAS-2B cells were grown in LHC-9 media. Human TRPV3 over-expressing BEAS-2B cells (TRPV3-OE) were created by transfecting BEAS-2B cells with a pcDNA3.1-TRPV3-V5/His expression plasmid. TRPV3-OE cells were selected using Geneticin (300 $\mu g/mL$); individual colonies were isolated, expanded, and subsequently screened for increased TRPV3 agonist-induced calcium flux and TRPV3 mRNA and protein expression. Data illustrating TRPV3 over-expression in the TRPV3-OE cells used in this study are collected in Supplementary Figure 1. Normal human bronchial epithelial cells (NHBE; donor IDs 14664, 31442, and 9999-1) were purchased from Lonza (Walkersville, MD). Human lobar bronchial epithelial cells (Lobar; donor ID 01344) were purchased from Lifeline Cell Technology (Frederick, MD). All primary cells were maintained for no more than five passages according to supplier recommendations.

Calcium Imaging Assays. Calcium flux/TRPV3 activity was assayed using the Fluo-4 Direct assay kit (Invitrogen). Treatment-induced changes in cellular fluorescence were quantified from fluorescence micrographs

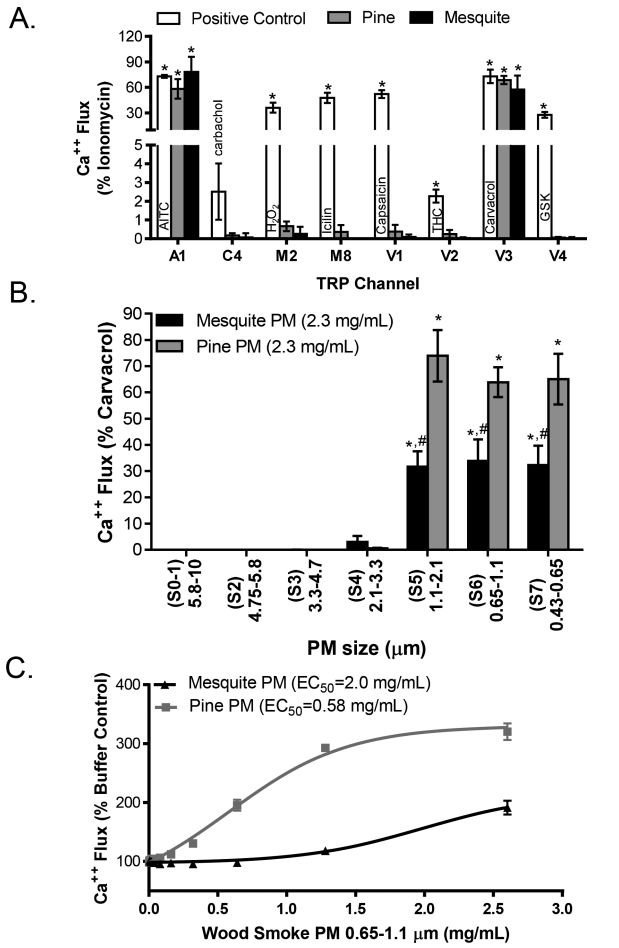

Figure 1. (A) TRP channel activation/calcium flux data for TRP-specific/positive control agonists (white), pine PM (gray; 0.73 mg/mL, 57 $\mu g/cm^2$), and mesquite PM (black; 0.73 mg/mL, 57 $\mu g/cm^2$) in TRP channel over-expressing HEK-293 cells. Data are normalized to ionomycin (10 μM). Positive controls for each channel include TRPA1-AITC (150 μM), TRPC4-carbachol (750 nM), TRPM2-H_2O_2 (1 mM), TRPM8-icilin (20 μM), TRPV1-capcascin (20 μM), TRPV2-THC (100 μM), TRPV3-carvacrol (300 μM), TRPV4-GSK (25 nM). *, statistically significant responses ($p < 0.05$) relative to vehicle controls, determined by the analysis of each cell type individually using one-way ANOVA and a Dunnett post-test ($\alpha = 0.05$). (B) Calcium flux data for different size fractions (Anderson Cascade impactor stages 0−7 (S0−7)) of pine and mesquite smoke PM (0.73 mg/mL; 57 $\mu g/cm^2$), normalized to the positive control for TRPV3 (carvacrol; 300 μM). *, Statically significant responses ($p < 0.05$) relative to vehicle controls; #, statistically significant responses ($p < 0.05$) relative to pine as determined using a two-way ANOVA using and the Bonferonni post-test. (C) EC_{50} values for TRPV3 activation by pine and mesquite PM (0.65−1.1 μm) in TRPV3-over-expressing HEK-293 cells. Data were collected using a BMG Labtech NOVOstar plate reader and are represented as the mean ± standard error of the mean ($n \geq 3$).

DOI: 10.1021/acs.chemrestox.7b00336
Chem. Res. Toxicol. 2018, 31, 291−301

or using a NOVOStar fluorescence plate reader (BMG Labtech; Offenberg, Germany), as previously described.[30−34] All agonist treatment solutions were prepared in LHC-9 at 3× concentration and added to cells at 37 °C. Particles were added based on the surface area of the vessel ($\mu g/cm^2$). Data from HEK-293 TRP-over-expressing cells were corrected for non-specific responses, if any, observed with HEK-293 cells. Data were also either normalized to the maximum attainable change in fluorescence elicited by ionomycin (10 μM) post-treatment or to the change elicited by a maximum stimulatory concentration of a positive control agonist, as noted in the figure legends.

Identification of Novel TRPV3 Agonists in PM. Analysis of chemical components comprising the various PM samples was performed at the University of Utah Metabolomics Core facility. Assays were performed on a Waters GCT Premier mass spectrometer fitted with an Agilent 6890 gas chromatograph and a Gerstel MPS2 auto sampler. Samples in DMSO (approximately 10 mg/mL) were diluted to 1 mg/mL in pyridine and then transferred to auto sampler vials, and 1 μL of the sample was injected into the inlet held at 250 °C using split mode at a 10:1 split ratio. The gas chromatograph had an initial temperature of 95 °C for 1 min followed by a 40 °C/min ramp to 110 °C and a hold time of 2 min. This was followed by a second 5 °C/min ramp to 250 °C, a third ramp to 350 °C, then a final hold time of 3 min. A 30 m Restek Rxi-5 MS column with a 5 m guard column was employed for chromatographic separation. Data were collected using MassLynx 4.1 software (Waters) and a text file containing the area under the curve for all of the analyte peaks was generated. Principle component analysis (PCA) and partial least-squares discriminate analysis (PLS-DA) was performed either using SIMCA-P 12.0 (Umetrics, Kinnelon, NJ) or Metaboanalyst 3.0 (http://www.metaboanalyst.ca/). Analytes showing high correlation with TRPV3 potency were preliminarily identified via spectral matching using the GC-EIMS (NIST 08) spectral database, and subsequent comparisons to purchased standards. The potency and selectivity of the potential TRPV3 agonists was determined by quantifying TRP channel activation (Ca^{2+} flux) in HEK-293 and/or BEAS-2B TRP channel over-expressing cells, as described above. Additional confirmations of agonists and quantification of selected analytes in WBSPM was performed using an Agilent GC-MSD equipped with a 30 m DB-5 MS (0.25 μm i.d.; 0.25 μm film thickness) column. For quantification the following assay parameters were used: extracts were diluted to 1 mg/mL in methylene chloride, transferred to auto sampler vials, and 4 μL of the sample was injected into the inlet held at 300 °C using splitless mode. The gas chromatograph had an initial temperature of 55 °C for 0.5 min followed by a 10 °C/min ramp to 225 °C, followed by a 50 °C/min ramp to 325 °C, and a hold time of 5 min. Samples were assayed in either scan mode to identify new analytes or SIM mode using m/z values of 108 (cresols), 122 (xylenols), 146 (5,8-dihydro-1-naphthol), and 206 (2,4-di-*tert*-butylphenol/internal standard).

Acute Cytotoxicity Assay. Cytotoxicity assays were performed in 96-well plates with 24 h incubations and assessment of residual cell viability using the Dojindo Cell Counting Kit 8 (Dojindo; Rockville, MD). Cells were plated 24−48 h prior to treatment and were treated at 85−90% confluence.

qPCR Gene Expression. A549, BEAS-2B, and Lobar cells were cultured in 25 cm^2 flasks. Three passages for each cell type were collected for biological replicates. NHBE cells from three donor samples were cultured in 12-well plates. At 80% confluence, cells were harvested and total RNA was isolated using the GenElute Mammalian Total RNA Miniprep Kit (Sigma; St. Louis, MO). Total RNA (1 μg) was converted to cDNA using iScript Reverse Transcription Supermix (BioRad; Hercules, CA). The cDNA was diluted 1:1 for analysis by quantitative real-time PCR (qPCR) using a Life Technologies QuantStudio 6 Flex instrument and the TaqMan probe-based assays for human TRPV3 (Hs00376854_m1) and human TRPA1 (Hs00175798_m1). Values for TRPA1 and TRPV3 were normalized to β2-macroglobulin (β2M; Hs00984230_m1) and quantification TRP channel mRNA expression was calculated using a standard curve.

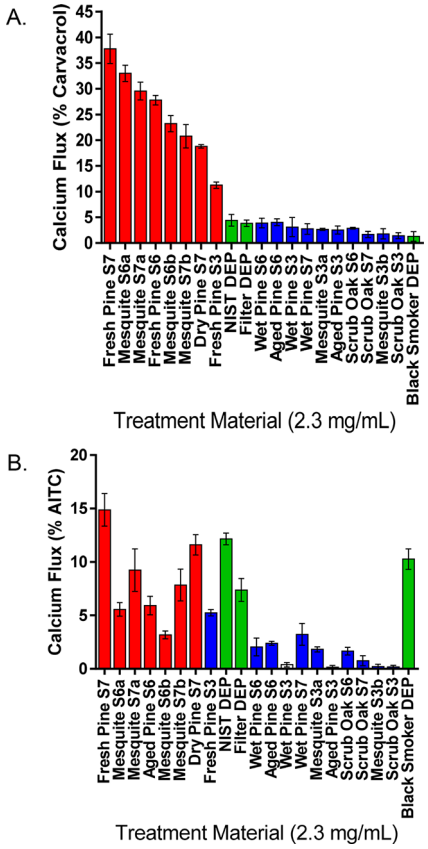

Figure 2. (A) Calcium flux in TRPV3-over-expressing HEK-293 cells treated with various PM at 0.73 mg/mL; 57 $\mu g/cm^2$), normalized to carvacrol (300 μM). Red is used to indicate the high potency wood smoke PM samples, green are the DEP extracts, and blue is low potency wood smoke PM. Different size fractions of the WSPM is represented by size/impactor stage number (S0−7) as defined in Figure 1B. These three categories were used for grouping and PCA + PLS-DA analysis in Figure 3. (B) Calcium flux in TRPA1-over-expressing HEK-293 cells treated with various PM at 0.73 mg/mL; 57 $\mu g/cm^2$), normalized to allyl-isothiocyanate (150 μM). The color scheme and order of PM is the same as panel A to facilitate comparisons between TRPV3 and TRPA1 activation by the same materials.

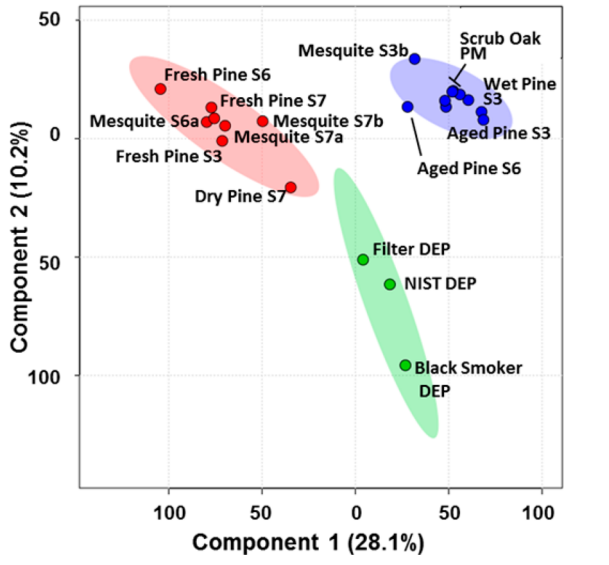

Figure 3. PLS-DA scores plot showing the relationship between PM potency and GC/MS chromatographic components shared among the most potent wood smoke PM (red), least potent wood smoke PM (blue), and DEP (green). Data analysis and graphics were generated using Metaboanalyst 3.0.

DOI: 10.1021/acs.chemrestox.7b00336
Chem. Res. Toxicol. 2018, 31, 291−301

TRPV3 Western Blot. Protein was isolated from cells using RIPA lysis buffer (Thermo Scientific; Rockford, IL) supplemented with Halt protease inhibitor cocktail (Thermo Scientific; Rockford, IL). The cell lysate was sonicated at 50% amplitude for 2 s, three times, and centrifuged at 12000*g* for 5 min. Protein concentration was measured using the BCA assay (Pierce; Rockford, IL). Total protein lysate obtained from TRPV3-OE BEAS-2B cells was used as a positive control (0.25 μg/lane). Protein (25 μg) was loaded into a 4−12% Bis-Tris gel (Thermo Scientific; Rockford, IL). TRPV3 protein expression was assessed using a TRPV3 mouse primary antibody (75-043; NeuroMab; Davis, CA (1:1000)) and a donkey anti-mouse HRP secondary antibody (NA931VS; GE Healthcare Lifesciences (1:10000)). Protein expression/band density was quantified using Image-J and normalized to total protein from amido black post-stained membranes as previously described.[35] The TRPV3 band was observed at ∼90 kDa.

RNA Sequencing. RNA sequencing was performed by the High Throughput Genomics Core Facility at the Huntsman Cancer Institute, University of Utah. BEAS-2B and TRPV3-OE BEAS-2B cells were harvested using trypsin and total RNA was isolated using the RNeasy mini kit with on column DNase I digestion (Qiagen). RNA quality was assessed by RNA nanochip technology and library construction was performed using the Illumina TruSeq Stranded mRNA Sample Preparation kit using established protocols. The sequencing libraries (18 pM) were then chemically denatured and applied to an Illumina TruSeq v3 single-read flow cell using an Illumina cBot. Hybridized molecules were clonally amplified and annealed to sequencing primers with reagents from an Illumina TruSeq SR Cluster Kit v3-cBot-HS (GD-401-3001). Following transfer of the flow cell to an Illumina HiSeq instrument (HCS v2.0.12 and RTA v1.17.21.3), a 50-cycle single-read sequence run was performed using TruSeq SBS v3 sequencing reagents (FC-401-3002). Raw data were processed by the University of Utah Bioinformatics core to quantify differential mRNA expression between the two cell types. The data presented in this publication have been deposited in NCBI's Gene Expression Omnibus[36] and are accessible through GEO Series accession number (GSE109598).

Mice. Experimental protocols were approved by the University of Utah Animal Care and Use Committee. Male C57BL/6 mice (Jackson Laboratories (20−25 g; 6−8 weeks old)) were used. Mice were housed in an AAALAC-approved vivarium maintained with 12 h/12 h light/dark cycles, at 23−26 °C and 40−50% relative humidity. Standard lab chow and water were provided *ad libitum*. Fresh pine PM (resuspended daily in DMSO) was dosed at 0.5 mg/kg (12.5 μg total PM/dose) every

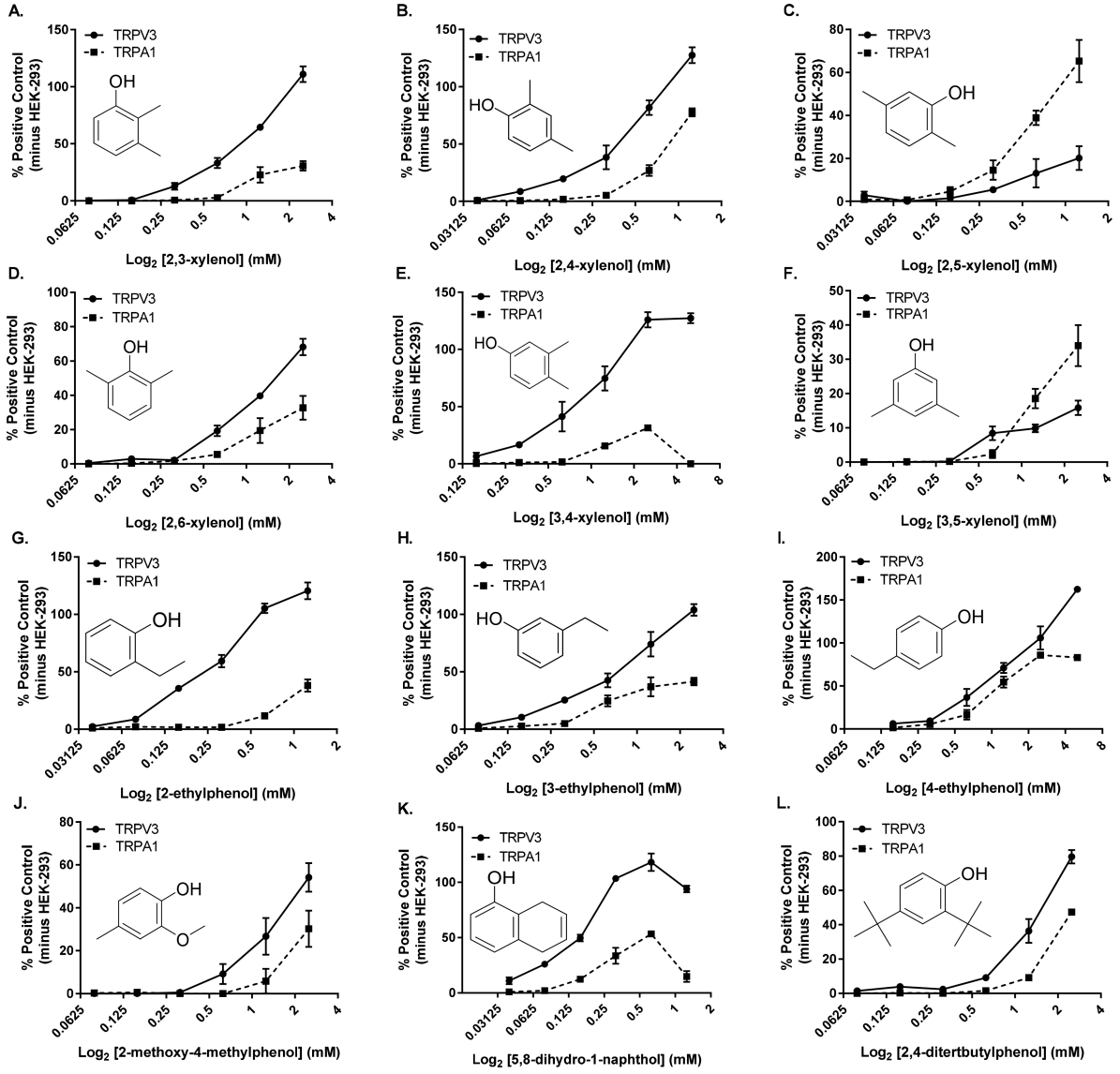

Figure 4. Dose−response relationships for the activation of human TRPA1 and TRPV3 channels over-expressed in HEK-293 cells by chemicals identified in WBSPM. Data are the mean and SEM for $n \geq 3$ replicates. (A) 2,3-xylenol, (B) 2,4-xylenol, (C) 2,5-xylenol, (D) 2,6-xylenol, (E) 3,4-xylenol, (F) 3,5-xylenol, (G) 2-ethylphenol, (H) 3-ethylphenol, (I) 4-ethylphenol, (J) 2-methoxy-4-methylphenol, (K) 5,8-dihydro-1-naphthol, and (L) 2,4-di-*tert*-butylphenol.

DOI: 10.1021/acs.chemrestox.7b00336
Chem. Res. Toxicol. 2018, 31, 291−301

other day via the oropharyngeal route, with analysis and necropsy 24 h after the third dose. The dosing scheme is illustrated in Figure 11A and is similar to that reported by Nemmar et al. using diesel exhaust PM.[37] The 0.5 mg/kg dose (12.5 μg of $PM_{1.1-2}$) corresponds to the amount PM collected from burning 6−7 mg of pine. This dose represents an approximate area dose of 10−20 ng/cm^2, estimated using an surface area of 600 cm^2 for an adult mouse lung,[38] and assuming 50−100% delivery and retention of the oropharyngeal dose in the lungs. This dose roughly approximates the 2−25 ng/cm^2 area dose that is predicted if a human were exposed to WBSPM at 5000 μg/m^3 for 8−24 h/day assuming a lung surface area of 70 m^2 and exchange of ∼458 L of air/h with 10−30% deposition throughout the respiratory tract for adult humans. This level of exposure for humans is on the high side, but plausible, and represents a scenario for which acute adverse responses and effects on human health have been reported.[1,2] Mice receiving the TRPV3 antagonist were injected i.p. (150 μL) with 1 mg/kg antagonist diluted from a DMSO stock in saline (DMSO = 1%) 1 h before pine exposure. Additionally, mice were co-treated with 1 μM TRPV3 antagonist diluted in the pine PM suspensions (DMSO = 1%) via the oropharyngeal route.

Pulmonary Mechanics. Airway resistance, compliance, and elastance were measured in anesthetized (ketamine + xylazine 100 + 20 mg/kg), paralyzed (0.1 mg/kg vecuronium bromide), and tracheostomized mice using a computer controlled small animal ventilator (Flexivent FX1; SCIREQ Inc., Montreal, Qc, Canada) as previously described.[39] Baseline measurements were collected for each mouse followed by assessment of bronchial reactivity/contractility elicited by serial delivery of increasing concentrations of aerosolized methacholine using the Flexivent Aeroneb fine particle nebulizer (0, 3.125, 6.25, 12.5, 25, and 50 mg/mL) in saline for 10 s per dose at 4−5 min intervals. The area under the curve value for measured criteria was calculated at each methacholine dose using a single-compartment model to generate methacholine dose−response curves. Each treatment group consisted of five age-matched mice.

Statistical Analysis. Values generally represent the mean ± SEM. One-way or two-way ANOVA with post-testing at the 95% confidence interval was used to determine significance, as indicated in each figure legend.

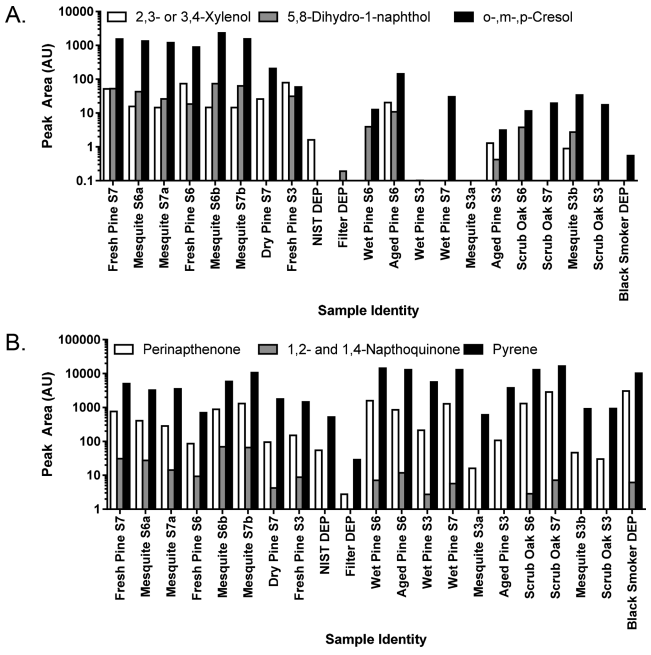

Figure 5. (A) Relative peak areas for GC/MS peaks preliminarily identified as 2,3- and/or 3,4-xylenol (white bars), 5,8-dihydro-1-naphthol (gray bars), and *o*-, *m*-, and/or *p*-cresol (black bars) for each of the samples tested as TRPV3 agonists and assayed by PCA + PLS-DA. (B) Relative peak areas for the chemicals perinaphthenone (white bars; a TRPA1 agonist), 1,2- and 1,4-naphthoquinone (gray bars; also TRPA1 agonists), and a common PAH pyrene (black bars).

RESULTS

TRP Channel Activation by Pine and Mesquite Wood Smoke PM. Human TRP channel activation by pine and mesquite PM was evaluated. HEK-293 cells over-expressing TRPA1, C4, M2, M8, V1, V2, V3, or V4 were treated with pine and mesquite PM (0.65−1.1 μm) at 0.73 mg/mL (equivalent to 57 μg/cm^2), and positive controls for each TRP channel. Ca^{2+} flux was observed in TRPA1 and TRPV3-over-expressing cells (Figure 1A). The calcium response in these cells was comparable in both rate and magnitude to the respective positive controls (TRPA1 = AITC at 150 μM and TRPV3 = carvacrol at 300 μM). Activation of TRPA1 by pine and mesquite PM was previously reported by our group,[30] but TRPV3 activation was novel. Analysis of TRPV3 activation by pine and mesquite PM of different size ranges (0.43 → 10 μm; stages 0−7 of on the Anderson cascade impactor) demonstrated that PM < 2.1 μm (stages 5−7 on the Anderson

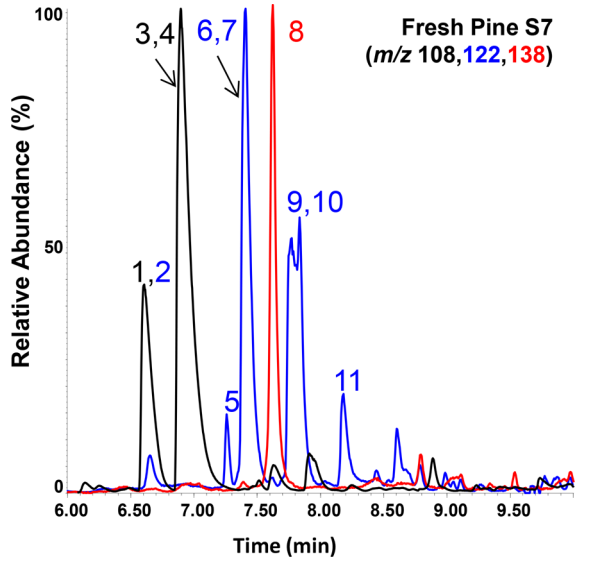

Figure 6. Extracted ion chromatogram highlighting the presence of cresol (black trace; numbers 1, 3, and 4), xylenols and ethyl phenols (blue trace; numbers 2, 5, 6, 7, 9, 10, and 11), and 2-methoxy-4-methylphenol (red trace; number 8). The reader is referred to Table 1 for additional details regarding the identification of and GC-MS characteristics of these compounds.

Table 1. Summary of GC/MS Analysis of Pine Particulate Matter, Highlighting the Cresol and Xylenol Analogues as Well as 2-Methoxy-4-methylphenol in the Chromatogram[a]

chemical name	number on chromatogram in Figure 6	retention time (min); *m/z*	match quality score[b]
2-methyphenol (*o*-cresol)	1	6.7; 108	86
2,6-dimethylphenol (xylenol)	2	6.7; 122	47
3- and/or 4-methyphenol (*m*-, *p*-cresol)	3, 4	6.9; 122	90/86
2- and/or 3-ethylphenol	5	7.3; 122	72/72
2,4- and/or 2,5-dimethylphenol (xylenol)	6, 7	7.4; 108	91/87
2-methoxy-4-methylphenol	8	7.6; 138	90
4-ethylphenol	9	7.7; 122	86
2,3- and/or 3,5-dimethylphenol (xylenol)	10	7.8; 122	91/91
3,4-dimethylphenol (xylenol)	11	8.2; 122	72

[a]Retention times, *m/z* values, and spectra were verified relative to authentic standards. [b]From NIST08 Library.

DOI: 10.1021/acs.chemrestox.7b00336
Chem. Res. Toxicol. 2018, 31, 291−301

cascade impactor) were most potent (Figure 1B). Furthermore, pine PM was more potent on a mass basis than mesquite PM (Figure 1B,C).

Characteristics of TRPV3 and TRPA1 Activation by Different WBSPM Samples. PM was collected from burning fresh cut, wet, aged, and dry pine; mesquite wood chips (two separate burnings denoted by "a" and "b"), and scrub oak. Ethanol extracts of three different diesel exhaust particle samples were also prepared. An equal mass of each material (2.3 mg/mL equivalent to 180 $\mu g/cm^2$) was applied to TRPV3-over-expressing HEK-293 cells and Ca^{2+} flux was quantified (Figure 2A). PM < 2.1 μm (stages 5−7 of the cascade impactor) from fresh pine and mesquite wood were the most potent TRPV3 agonists. Specific activation of TRPV3 was not observed with extracts of the DEP materials, pine and mesquite PM > 5 μm (stages 0−2 of the cascade impactor), or scrub oak PM. Of significance, the relative activity of these wood smoke and DEP extract materials differed from TRPA1 (Figure 2B), suggesting differences in the relative abundance of TRPA1 and V3 agonists in these materials.

Identification of TRPV3 Agonists in Wood Smoke PM. The chemical basis for TRPV3 activation by WBSPM was further explored. Equal quantities of materials from Figure 2 were assayed by high-resolution GC/MS and the chromatographic and spectral data processed using principal component analysis (PCA) and partial least-squares discriminant analysis (PLS-DA) (Figure 3). The most potent TRPV3 activating WBSPM (red), the essentially inactive WBSPM (blue), and DEP samples (green) clustered as independent groups based on similarities/differences in their chemical compositions (A heat map illustrating the chemical diversity, similarities, and differences is shown as Supplementary Figure 2). A list of chemicals associated with the most potent TRPV3 activating PM was generated by matching the EI mass spectra with entries in the NIST08 database (Supplementary Table 1).

Candidate molecules were then purchased and screened for TRPV3 agonist activity in hTRPV3-over-expressing HEK-293 cells (see Supplementary Table 1 for a summary of the compounds assayed). In our initial screens, three compounds activated TRPV3: 2,3-xylenol, 3,4-xylenol, and 5,8-dihydronaphthol (Figure 4). Of note, 2,5-xylenol was known to be a TRPV3 agonist.[40] Relative GC/MS peak areas of 2,3- and 3,4-xylenol (combined), *o*-, *m*-, *p*-cresol (combined), and 5,8-dihydro-1-naphtol across the various WBSPM samples are shown in Figure 5A; those of the TRPA1 agonists perinaphthenone, 1,2- and 1,4-naphthoquinone (combined), and the polycyclic aromatic hydrocarbon (PAH) pyrene (used as a general comparator) are shown in Figure 5B.

Quantification of TRPV3 Agonists in Pine and Mesquite PM. The concentrations of 2,3-, 2,4- and/or 2,5- and 3,4-xylenol in pine and mesquite PM (0.43−2.1 μm) were 0.3, 0.3, and 0.03% by weight (μg/mg total PM). The concentration of 5,8-dihydro-1-naphthol was 0.03%. A GC-MS extracted ion chromatogram from quantitative analysis of pine PM (0.65−1.1 μm) is shown in Figure 6, highlighting the presence of multiple cresol (numbers 1, 3, and 4) and xylenol (numbers 2, 6, 7, 10, and 11) analogues, and analytes not previously identified using the metabolomics approach; 2- and/or 3-, and 4-ethyl phenol (numbers 5 and 9), and 2-methoxy-4-methylphenol (number 8). Table 1 summarizes the chromatographic and spectral match criteria used to identify these components, while Figure 4 shows the structures and potency for the various substances tested as TRPV3 and TRPA1 agonists. To summarize, cresol analogues did not activate TRPV3. Xylenol and ethylphenol analogues activated TRPV3 with slightly different potency and relative selectivity for TRPV3 versus TRPA1. Additionally, 2,4-di-*tert*-butylphenol, previously identified as a TRPA1 agonist in the "black smoker" DEP, was a TRPV3 agonist.

TRPV3 Expression and Function in Lung Cells. TRPV3 expression in primary bronchial epithelial cells[41] and lung cancer cells[42] has been reported. Here, the expression of TRPV3 mRNA in A549, BEAS-2B, Lobar bronchial, and NHBE cells was quantified by qPCR (Figure 7A) and Western blot (Figure 7B). TRPV3 protein expression was observed in A549, BEAS-2B, Lobar, and NHBE cells, which was confirmed by functional studies (Figure 7C). TRPV3 activity was observed in A549 and Lobar bronchial cells, and to a lesser extent in NHBE and BEAS-2B cells using

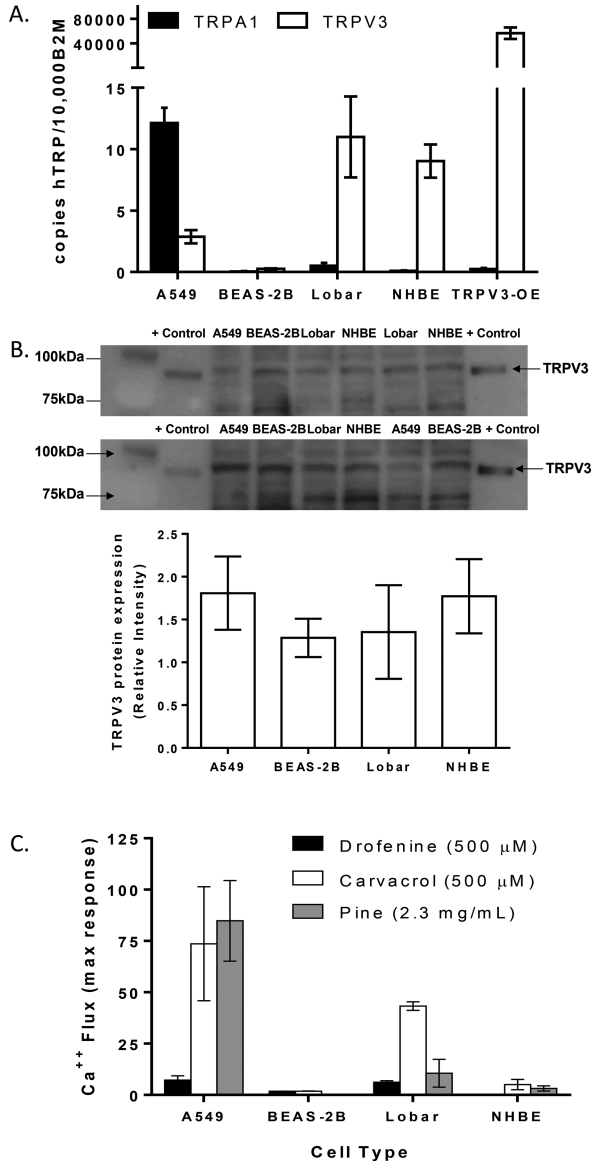

Figure 7. (A) mRNA expression data for TRPA1 and TRPV3 in human lung epithelial cell lines. (B) Protein expression data for TRPV3 in human lung epithelial cells. BEAS-2B TRPV3-OE cells are used as a positive control producing a band at ~90 kDa. Each bar for both protein and mRNA represents three biological replicates over three passages. NHBEs are from three different donors. (C) Ca^{2+} flux in response to various TRPA1 and TRPV3 agonists in human lung epithelial cells. Drofenine is selective for TRPV3, while pine PM and carvacrol activate both TRPA1 and TRPV1. Data are the mean and SEM for $n = 3$ replicates.

DOI: 10.1021/acs.chemrestox.7b00336
Chem. Res. Toxicol. 2018, 31, 291−301

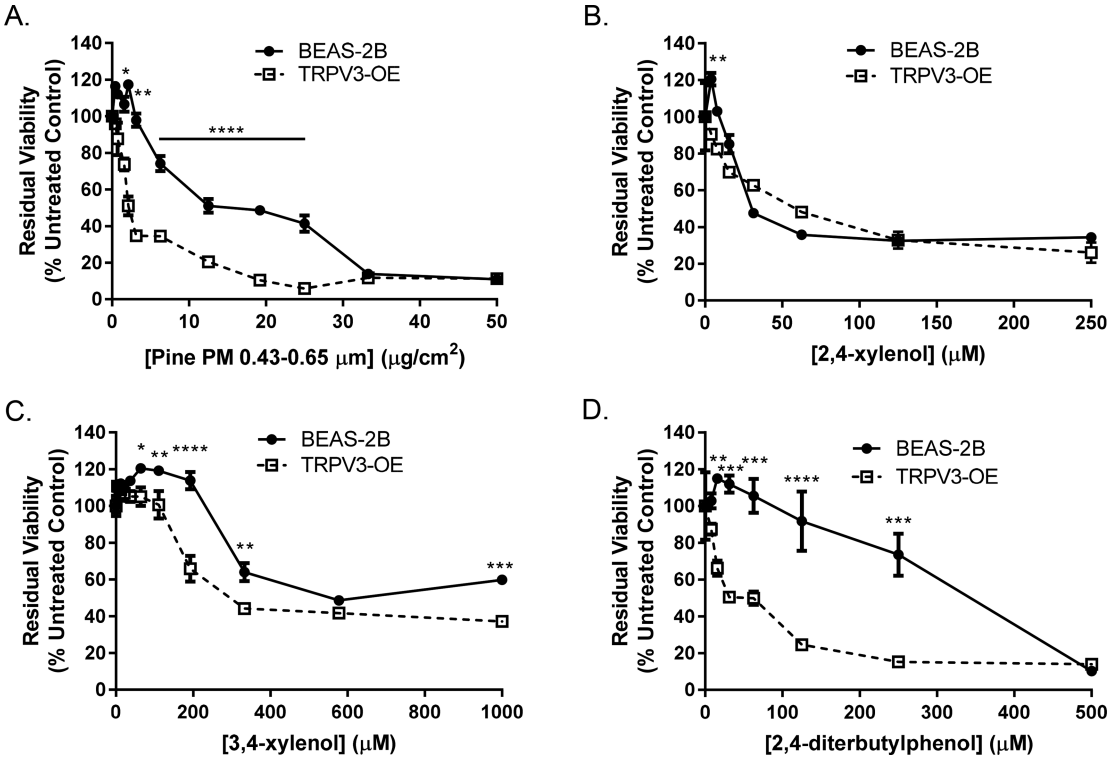

Figure 8. Cytotoxicity data for (A) pine PM (0.43−0.65 μm), (B) 2,4-xylenol, (C) 3,4-xylenol, and (D) 2,4-di-*tert*-butylphenol in BEAS-2B and TRPV3-OE BEAS-2B cells. Data represent the mean and SEM from $n \geq 4$ replicates from two independent experiments. Statistical analysis was determined by 2-way ANOVA using and the Bonferonni post-test. *indicates $p < 0.05$, **$p < 0.01$, ***$p < 0.001$, and **** $p < 0.001$.

drofenine, carvacrol, and pine PM as TRPV3 agonists (Figure 7C). Note, drofenine activates TRPV3, but not TRPA1,[31] while both carvacrol and pine PM activate TRPV3 and TRPA1. Additionally, NHBE cells do not perform as well in calcium assays and therefore minimal calcium flux was observed. These data show that both TRPV3 and A1 likely contribute to the responses of these cells to pine PM, with the relative contribution being determined by the relative levels of expression of these channels in the specific cell type.

Cytotoxicity of WBSPM and Pure TRPV3 Agonists in Lung Cells. The LD_{50} for pine PM was 18 $\mu g/cm^2$ in BEAS-2B cells and 3 $\mu g/cm^2$ in TRPV3-OE BEAS-2B cells (Figure 8A). In A549 cells, the EC_{50} for pine and mesquite PM were 35 and >100 $\mu g/cm^2$, 11 and 10 $\mu g/cm^2$ in NHBE cells, and 13 $\mu g/cm^2$ for pine PM in Lobar cells (data not shown). TRPV3 overexpression also increased the cytotoxicity of 3,5-xylenol and 2,4-di-*tert*-butylphenol, but not 2,4-xylenol (Figures 8B−D).

Relative Role of TRPV3 in WBSPM Cytotoxicity. Because pine PM and the pure TRPV3 agonists in WBPSM also activate TRPA1, the relative roles for TRPV3 and TRPA1 were further explored. Transcriptomic analysis of BEAS-2B and TRPV3-OE BEAS-2B cells revealed an up-regulation of TRPA1 and TRPV4 in the TRPV3-OE cells; TRPV1 expression was unchanged (Figure 9). BEAS-2B and TRPV3-OE BEAS-2B cells were subsequently treated with LD_{50} concentrations of pine PM in the presence of increasing concentrations of the following TRP channel antagonists: HC-030031 (TRPA1), LJO-328 (TRPV1), 2-(5-trifluoromethylpyridin-2-ylsulfanyl)-1-(8-methyl-3,4-dihydro-2*H*-quinolin-1-yl)-ethanone (TRPV3), and HC-067047 (TRPV4) (Figure 10A−D). Inhibition of TRPA1, V1, and V4 failed to reduce the cytotoxicity of pine PM, but inhibition of TRPV3 afforded partial protection in both BEAS-2B and TRPV3-OE cells (note: the TRPV3 antagonist was also cytotoxic at concentrations above 20−30 μM).

Role of TRPV3 in Bronchial Hypersensitivity. Treatment of mice with 0.5 mg/kg pine PM (0.43−1.1 μm) via oropharyngeal aspiration every other day for 6 days, increased airway sensitivity to acute methacholine challenge. Dosing scheme is shown in Figure 11A. Changes in airway resistance as a function of methacholine dose and treatment with either pine PM, alone or in combination with a TRPV3 antagonist, is summarized in Figure 11B,C. Pre- and co-treatment of mice with the TRPV3 antagonist attenuated the increase in sensitivity to methacholine and changes in airway resistance suggesting a role for TRPV3 in the development of sub-acute airway hypersensitivity to methacholine.

DISCUSSION

This study characterized TRPV3 in lung cells, its activation by selected wood smoke particles and specific chemical constituents thereof, and responses of lung cells and lungs of mice as a function of TRPV3 activity. The results provide new insight into the roles of TRPV3 in lung epithelial cells and evidence supporting a relationship between TRPV3 and some of the known, but mechanistically undefined, pneumotoxic properties that have been reported previously for WBSPM.

Environmental PM is physically and chemically diverse. The precise composition of combustion-generated PM varies by origin, combustion conditions, age, and other factors. Consequently, the biological sensors that detect PM in the airways, and the effects that PM has on lung cells/tissue, can vary. Figure 1 shows that TRPA1 and TRPV3 were activated by pine and mesquite PM. Activation of TRPV3 by WBSPM was not universal for all forms of WBSPM but it was unique from TRPA1, ultimately shown to be driven by specific chemicals occurring in only certain types of PM; notably, pine and mesquite PM < 2.1 μm containing xylenols, ethyl phenols, 2-methoxy-4-methylphenol, and

DOI: 10.1021/acs.chemrestox.7b00336
Chem. Res. Toxicol. 2018, 31, 291−301

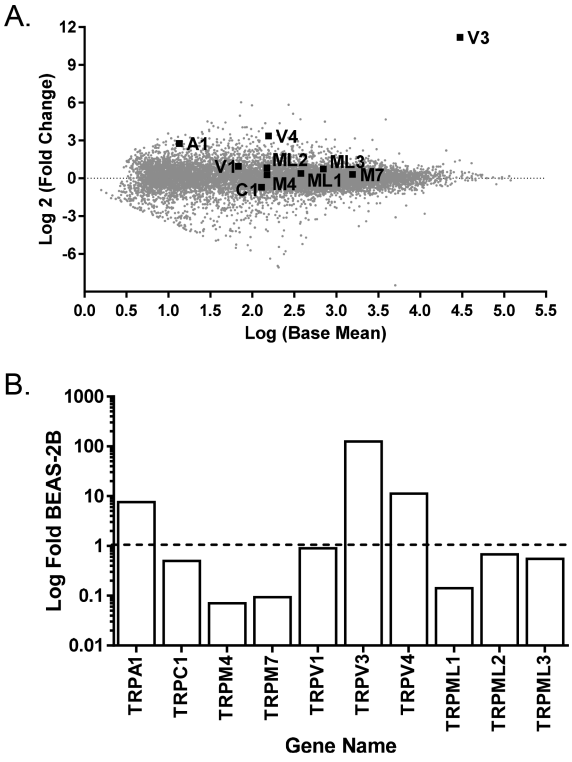

Figure 9. (A) Log ratio/mean average plot of mRNA sequencing data comparing the basal expression of TRP genes as a function of TRPV3 over-expression. TRP channel genes are highlighted in blue with features appearing at values >0 being over-expressed in TRPV3-OE BEAS-2B cells relative to BEAS-2B cells. (B) Graphical representation of fold changes in TRP gene mRNA expression. All data points represent averages from duplicate sequencing runs.

5,8-dihydronapthol (Figures 2–6; Table 1). While it is likely that other TRPV3 agonists exist in the pine and mesquite PM, as well as in other forms of environmental WBSPM that humans may be exposed to, these results link the presence of specific chemicals to the activation of a novel biological target. These results also further underscore the concept that the biological effects of a given form of PM are highly dependent upon the chemical composition of the PM, and the ability of specific chemicals to interact with and activate explicit biological sensors and pathways.

A characteristic adverse effect of WBSPM inhalation is lung epithelial cell cytotoxicity.[43,44] Indeed, both pine and mesquite PM were cytotoxic to a variety of lung cells in which TRPV3 was expressed (Figures 7 and 8). Both WBSPM and pure TRPV3 agonists were cytotoxic to lung epithelial cells and their toxicity involved TRPV3, with pine PM being attenuated by a TRPV3 antagonist (Figure 8 and 10). Interestingly, it was also found that TRPV3-OE BEAS-2B expressed higher levels of TRPA1 and TRPV4 (Figure 9). This was an intriguing finding since TRPA1 expression in BEAS-2B cells, and other similar lung cells, is typically low/non-detectable, with the exception that we have recently discovered that heterozygosity for the TRPV1 I585V polymorphism (rs8065080) is associated with increased TRPA1 expression in NHBE cells, and perhaps increased sensitivity to environmental pollutants.[35] Of note, the NHBE cells used in this study expressed wild-type TRPV1, and therefore expression of TRPA1 mRNA was not detected (Figure 7A). Regardless, the results in Figures 8–10 prompted us to investigate whether TRPA1 may also contribute to the acute cytotoxicity of pine PM and pure TRPV3 agonists, potentially explaining the heightened sensitivity of the TRPV3-OE cells to these materials. However, inhibition of TRPA1, as well as TRPV1, and TRPV4, did not

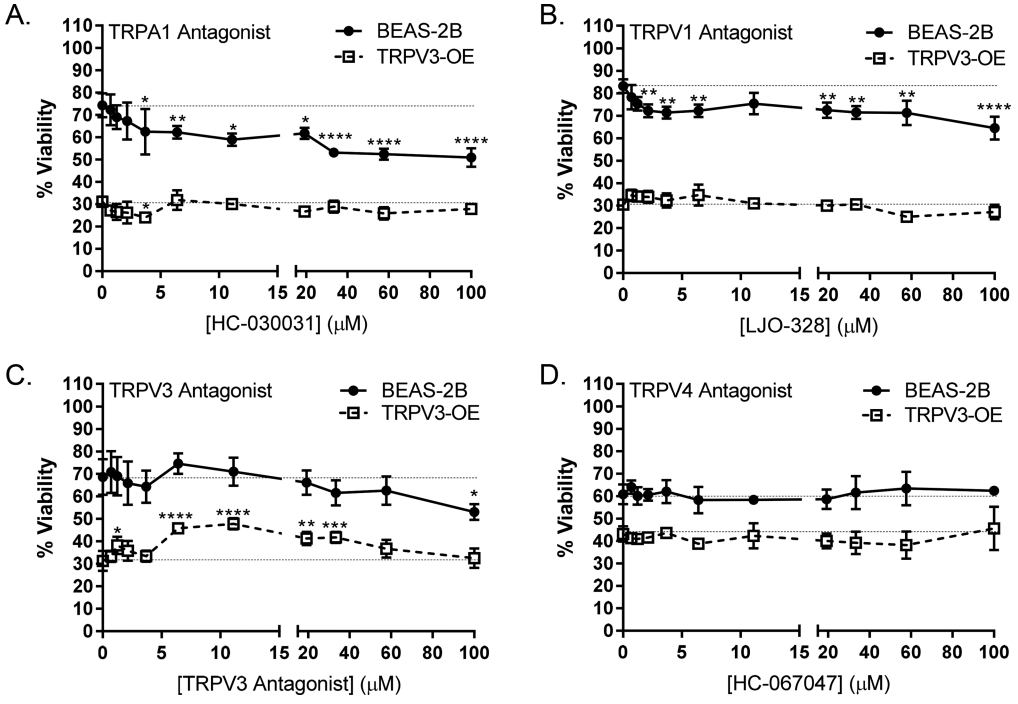

Figure 10. Inhibition of the cytotoxicity of pine PM (10 $\mu g/cm^2$) in BEAS-2B and in BEAS-2B TRPV3-OE cells using (A) the TRPA1 antagonist HC-030031, (B) the TRPV1 antagonist LJO-328, (C) The TRPV3 antagonist 2-(5-trifluoromethyl-pyridin-2-ylsulfanyl)-1-(8-methyl-3,4-dihydro-2*H*-quinolin-1-yl)-ethanone, and (D) the TRPV4 antagonist HC-067047. Data represent the mean and SEM from $n \geq 4$ replicates from two independent experiments. Statistical analysis was determined by two-way ANOVA using and the Bonferonni post-test. *, $p < 0.05$; **, $p < 0.01$; ***, $p < 0.001$; and ****, $p < 0.001$.

DOI: 10.1021/acs.chemrestox.7b00336
Chem. Res. Toxicol. 2018, 31, 291–301

protect cells from cytotoxicity indicating a prominent role for TRPV3 in mediating this outcome.

Like many types of inhaled PM, WBSPM affects the lungs. Relevant to this work, short-term exposure to WBSPM (PM10 ≥ 0.15−0.2 $\mu g/m^3$) has been shown to correlate with increased rates of hospital visits for respiratory complications, including the exacerbation of asthma and COPD.[9−18] We have previously identified TRPA1 as a target for WBSPM, specifically electrophiles present in these materials.[30] Activation of TRPA1 in the lungs has been shown to stimulate the cough reflex and bronchoconstriction, decrease respiratory drive, and promote neurogenic inflammation.[45] Gain of function polymorphisms in TRPA1 are also associated with poorer asthma control.[34] Thus, interactions between TRPA1 and WBSPM likely contribute to the acute irritant and pro-inflammatory effects of inhaled WBSPM. However, a role for TRPV3 has not yet been described.

Like TRPA1, TRPV3 expression has been reported to occur in TRPV1-positive dorsal root and trigeminal ganglia, and vagal afferent neurons, which are relevant to respiratory physiology.[46,47] Additionally, a certain amount of synergy appears to exist between TRPV3 and other TRP channels in these tissues. For example, Wu et al. suggest that while TRPV3 expression is lower than that of TRPV1, activation of TRPV3 may potentiate TRPV1 activation in vagal afferent neurons.[46] Intuitively, stimulation of TRPV3 in TRPV1-positive neurons and/or sensitization of TRPV1 should correlate with a stimulation of irritant responses similar to those described above for TRPA1. As such, this may be a mechanism by which WBSPM adversely affects the respiratory system. However, others have also reported that TRPV3 agonists, including thymol, have anti-tussive properties,[48] similar to menthol, which activates TRPM8 to attenuate responses to TRPA1 agonists.[48,49] Our data also suggest the possibility of interplay between TRPV3 expression/function and TRPA1 expression/function in epithelial cells, which could also affect the respiratory tract through a variety of mechanisms. Regardless, further investigation into the roles of TRPV3 in WBSPM pneumotoxicity is needed in order to fully understand the mechanistic basis for the results shown in Figure 11, that sub-acute pulmonary exposure of mice to pine PM sensitized mice to methacholine in an apparent TRPV3-dependent manner. While it remains unclear exactly how this sensitization occurs—whether it involved direct activation of TRPV3 in neurons or epithelial cells, changes in TRPA1, V3, or even V4 expression, cytotoxicity and loss of epithelial cells, inflammation, or other mechanisms—these data indicate a role for TRPV3 in the development of deleterious respiratory effects elicited by pine and perhaps other WBSPM.

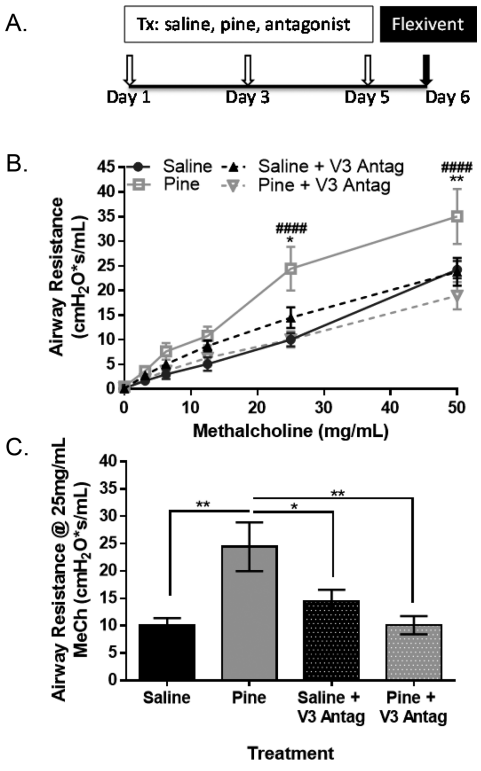

Figure 11. (A) Methacholine dose−response curves for changes in airway resistance in saline (black; $n = 5$), pine PM-treated (gray; $n = 5$), TRPV3-antagonist treated (dashed black; $n = 5$), and pine + TRPV3-antagonist cotreated (dashed gray; $n = 5$) C57BL/6 mice. Data are the mean ± standard error of the mean ($n = 5$). Data were analyzed by two-way ANOVA and a Bonferroni post-test comparing all groups: Differences compared to saline treatment are indicated as $p < 0.05$ (*), $p < 0.01$(**). (B) Comparison of changes in airway resistance at the 25 mg/mL methacholine dose. Data are the mean ± standard error of the mean ($n = 5$) and were analyzed by one-way ANOVA with a Newman−Keuls post-test; $p < 0.05$ (*), $p < 0.01$(**).

In summary, TRPV3 has been identified as a new molecular sensor for WBSPM in lung epithelial cells. The activation of TRPV3 is dependent upon the specific chemical composition of the WBSPM, suggesting that TRPV3 may play variable roles in WBSPM-induced pneumotoxicity, albeit varying as a function of the material being burned, the conditions used to burn the material, and other factors. Additionally, TRPV3 appears to play a role in determining lung cell and airway sensitivity to WBSPM. Accordingly, TRPV3 should be considered in future studies aimed at understanding mechanisms of lung injury and lung disorders and diseases associated with WBSPM exposures.

■ ASSOCIATED CONTENT

Supporting Information

The Supporting Information is available free of charge on the ACS Publications website at DOI: 10.1021/acs.chemrestox.7b00336.

Supplemental Figure 1, dose−response curves for activation of TRPV3 in BEAS-2B and TRPV3-OE BEAS-2B cells and EC_{50} values for drofenine and carvacrol in BEAS-2B and in BEAS-2B and TRPV3-OE BEAS-2B cells; Supplemental Figure 2, heat map comparing the overall GC-MS chemical signatures of various wood smoke and DEP samples; Supplementary Figure 3, Amido Black staining of Western blots used for normalization against total protein; and Supplemental Table 1, identities of compounds screened as TRPV3 agonists (PDF)

■ AUTHOR INFORMATION

Corresponding Author

*Phone: (801) 581-5236. Fax: (801) 585-5111. E-mail: chris.reilly@pharm.utah.edu.

ORCID

Cassandra E. Deering-Rice: 0000-0002-2103-1194

Funding

This work was funded by NIEHS grants ES017431 and ES027015. The High Throughput Genomics Core Facility at the Huntsman Cancer Institute, University of Utah, was partially supported by Award Number P30CA42014 from the National Cancer Institute.

Notes

The authors declare no competing financial interest.

DOI: 10.1021/acs.chemrestox.7b00336
Chem. Res. Toxicol. 2018, 31, 291−301

ABBREVIATIONS

TRPV1, Transient receptor potential vanilloid-1; TRPV2, transient receptor potential vanilloid-2; TRPV3, transient receptor potential vanilloid-3; TRPV4, transient receptor potential vanilloid-4; TRPA1, transient receptor potential ankyrin-1; TRPM2, transient receptor potential melastatin-2; TRPM4, transient receptor potential melastatin-4; TRPM7, transient receptor potential melastatin-7; TRPM8, transient receptor potential melastatin-8; TRPML1, transient receptor potential mucolipin-1; TRPML2, transient receptor potential mucolipin-2; TRPML3, transient receptor potential mucolipin-1; TRPC1, transient receptor potential canonical-1; PM, particulate material; WBSPM, wood/biomass smoke particulate material

REFERENCES

(1) Laumbach, R. J., and Kipen, H. M. (2012) Respiratory health effects of air pollution: update on biomass smoke and traffic pollution. *J. Allergy Clin. Immunol. 129*, 3−11 (quiz 12-13).

(2) Naeher, L. P., Brauer, M., Lipsett, M., Zelikoff, J. T., Simpson, C. D., Koenig, J. Q., and Smith, K. R. (2007) Woodsmoke health effects: a review. *Inhalation Toxicol. 19*, 67−106.

(3) Dogan, O. T., Elagoz, S., Ozsahin, S. L., Epozturk, K., Tuncer, E., and Akkurt, I. (2011) Pulmonary toxicity of chronic exposure to tobacco and biomass smoke in rats. *Clinics (Sao Paulo) 66*, 1081−1087.

(4) Lai, C. J., and Kou, Y. R. (1998) Stimulation of vagal pulmonary C fibers by inhaled wood smoke in rats. *J. Appl. Physiol. 84*, 30−36.

(5) Lal, K., Dutta, K. K., Vachhrajani, K. D., Gupta, G. S., and Srivastava, A. K. (1993) Histomorphological changes in lung of rats following exposure to wood smoke. *Indian J. Exp. Biol. 31*, 761−764.

(6) Barregard, L., Sallsten, G., Andersson, L., Almstrand, A. C., Gustafson, P., Andersson, M., and Olin, A. C. (2008) Experimental exposure to wood smoke: effects on airway inflammation and oxidative stress. *Occup. Environ. Med. 65*, 319−324.

(7) Stockfelt, L., Sallsten, G., Olin, A. C., Almerud, P., Samuelsson, L., Johannesson, S., Molnar, P., Strandberg, B., Almstrand, A. C., Bergemalm-Rynell, K., and Barregard, L. (2012) Effects on airways of short-term exposure to two kinds of wood smoke in a chamber study of healthy humans. *Inhalation Toxicol. 24*, 47−59.

(8) Ghio, A. J., Soukup, J. M., Case, M., Dailey, L. A., Richards, J., Berntsen, J., Devlin, R. B., Stone, S., and Rappold, A. (2012) Exposure to wood smoke particles produces inflammation in healthy volunteers. *Occup. Environ. Med. 69*, 170−175.

(9) Duclos, P., Sanderson, L. M., and Lipsett, M. (1990) The 1987 forest fire disaster in California: assessment of emergency room visits. *Arch. Environ. Health 45*, 53−58.

(10) Moore, D., Copes, R., Fisk, R., Joy, R., Chan, K., and Brauer, M. (2006) Population health effects of air quality changes due to forest fires in British Columbia in 2003: estimates from physician-visit billing data. *Can. J. Public Health 97*, 105−108.

(11) Mott, J. A., Mannino, D. M., Alverson, C. J., Kiyu, A., Hashim, J., Lee, T., Falter, K., and Redd, S. C. (2005) Cardiorespiratory hospitalizations associated with smoke exposure during the 1997, Southeast Asian forest fires. *Int. J. Hyg. Environ. Health 208*, 75−85.

(12) Mott, J. A., Meyer, P., Mannino, D., Redd, S. C., Smith, E. M., Gotway-Crawford, C., and Chase, E. (2002) Wildland forest fire smoke: health effects and intervention evaluation, Hoopa, California, 1999. *West. J. Med. 176*, 157−162.

(13) Schreuder, A. B., Larson, T. V., Sheppard, L., and Claiborn, C. S. (2006) Ambient woodsmoke and associated respiratory emergency department visits in Spokane, Washington. *Int. J. Occup. Environ. Health 12*, 147−153.

(14) Sutherland, E. R., Make, B. J., Vedal, S., Zhang, L., Dutton, S. J., Murphy, J. R., and Silkoff, P. E. (2005) Wildfire smoke and respiratory symptoms in patients with chronic obstructive pulmonary disease. *J. Allergy Clin. Immunol. 115*, 420−422.

(15) Long, W., Tate, R. B., Neuman, M., Manfreda, J., Becker, A. B., and Anthonisen, N. R. (1998) Respiratory symptoms in a susceptible population due to burning of agricultural residue. *Chest 113*, 351−357.

(16) Swiston, J. R., Davidson, W., Attridge, S., Li, G. T., Brauer, M., and van Eeden, S. F. (2008) Wood smoke exposure induces a pulmonary and systemic inflammatory response in firefighters. *Eur. Respir. J. 32*, 129−138.

(17) Norris, G., Larson, T., Koenig, J., Claiborn, C., Sheppard, L., and Finn, D. (2000) Asthma aggravation, combustion, and stagnant air. *Thorax 55*, 466−470.

(18) Norris, G., YoungPong, S. N., Koenig, J. Q., Larson, T. V., Sheppard, L., and Stout, J. W. (1999) An association between fine particles and asthma emergency department visits for children in Seattle. *Environ. Health Perspect 107*, 489−493.

(19) Noonan, C. W., Ward, T. J., Navidi, W., and Sheppard, L. (2012) A rural community intervention targeting biomass combustion sources: effects on air quality and reporting of children's respiratory outcomes. *Occup. Environ. Med. 69*, 354−360.

(20) Hu, G., Zhou, Y., Tian, J., Yao, W., Li, J., Li, B., and Ran, P. (2010) Risk of COPD from exposure to biomass smoke: a metaanalysis. *Chest 138*, 20−31.

(21) Kurmi, O. P., Semple, S., Simkhada, P., Smith, W. C., and Ayres, J. G. (2010) COPD and chronic bronchitis risk of indoor air pollution from solid fuel: a systematic review and meta-analysis. *Thorax 65*, 221−228.

(22) Po, J. Y., FitzGerald, J. M., and Carlsten, C. (2011) Respiratory disease associated with solid biomass fuel exposure in rural women and children: systematic review and meta-analysis. *Thorax 66*, 232−239.

(23) Regalado, J., Perez-Padilla, R., Sansores, R., Paramo Ramirez, J. I., Brauer, M., Pare, P., and Vedal, S. (2006) The effect of biomass burning on respiratory symptoms and lung function in rural Mexican women. *Am. J. Respir. Crit. Care Med. 174*, 901−905.

(24) Barry, A. C., Mannino, D. M., Hopenhayn, C., and Bush, H. (2010) Exposure to indoor biomass fuel pollutants and asthma prevalence in Southeastern Kentucky: results from the Burden of Lung Disease (BOLD) study. *J. Asthma 47*, 735−741.

(25) Mishra, V. (2003) Effect of indoor air pollution from biomass combustion on prevalence of asthma in the elderly. *Environ. Health Perspect. 111*, 71−77.

(26) Danielsen, P. H., Brauner, E. V., Barregard, L., Sallsten, G., Wallin, M., Olinski, R., Rozalski, R., Moeller, P., and Loft, S. (2008) Oxidatively damaged DNA and its repair after experimental exposure to wood smoke in healthy humans. *Mutat. Res., Fundam. Mol. Mech. Mutagen. 642*, 37−42.

(27) Danielsen, P. H., Loft, S., Jacobsen, N. R., Jensen, K. A., Autrup, H., Ravanat, J. L., Wallin, H., and Moeller, P. (2010) Oxidative Stress, Inflammation, and DNA Damage in Rats After Intratracheal Instillation or Oral Exposure to Ambient Air and Wood Smoke Particulate Matter. *Toxicol. Sci. 118*, 574−585.

(28) Danielsen, P. H., Loft, S., Kocbach, A., Schwarze, P. E., and Moeller, P. (2009) Oxidative damage to DNA and repair induced by Norwegian wood smoke particles in human A549 and THP-1 cell lines. *Mutat. Res., Genet. Toxicol. Environ. Mutagen. 674*, 116−122.

(29) Danielsen, P. H., Moeller, P., Jensen, K. A., Sharma, A. K., Wallin, H., Bossi, R., Autrup, H., Molhave, L., Ravanat, J. L., Briede, J. J., de Kok, T. M., and Loft, S. (2011) Oxidative Stress, DNA Damage, and Inflammation Induced by Ambient Air and Wood Smoke Particulate Matter in Human A549 and THP-1 Cell Lines. *Chem. Res. Toxicol. 24*, 168.

(30) Shapiro, D., Deering-Rice, C. E., Romero, E. G., Hughen, R. W., Light, A. R., Veranth, J. M., and Reilly, C. A. (2013) Activation of transient receptor potential ankyrin-1 (TRPA1) in lung cells by wood smoke particulate material. *Chem. Res. Toxicol. 26*, 750−758.

(31) Deering-Rice, C. E., Mitchell, V. K., Romero, E. G., Abdel Aziz, M. H., Ryskamp, D. A., Krizaj, D., Gopal, V. R., and Reilly, C. A. (2014) Drofenine: A 2-APB Analogue with Greater Selectivity for Human TRPV3. *Pharmacol. Res. Perspect. 2*, e00062.

(32) Deering-Rice, C. E., Romero, E. G., Shapiro, D., Hughen, R. W., Light, A. R., Yost, G. S., Veranth, J. M., and Reilly, C. A. (2011)

DOI: 10.1021/acs.chemrestox.7b00336
Chem. Res. Toxicol. 2018, 31, 291−301

Electrophilic components of diesel exhaust particles (DEP) activate transient receptor potential ankyrin-1 (TRPA1): a probable mechanism of acute pulmonary toxicity for DEP. *Chem. Res. Toxicol. 24*, 950−959.
(33) Deering-Rice, C. E., Johansen, M. E., Roberts, J. K., Thomas, K. C., Romero, E. G., Lee, J., Yost, G. S., Veranth, J. M., and Reilly, C. A. (2012) Transient receptor potential vanilloid-1 (TRPV1) is a mediator of lung toxicity for coal fly ash particulate material. *Mol. Pharmacol. 81*, 411−419.
(34) Deering-Rice, C. E., Shapiro, D., Romero, E. G., Stockmann, C., Bevans, T. S., Phan, Q. M., Stone, B. L., Fassl, B., Nkoy, F., Uchida, D. A., Ward, R. M., Veranth, J. M., and Reilly, C. A. (2015) Activation of Transient Receptor Potential Ankyrin-1 by Insoluble Particulate Material and Association with Asthma. *Am. J. Respir. Cell Mol. Biol. 53*, 893.
(35) Deering-Rice, C. E., Stockmann, C., Romero, E. G., Lu, Z., Shapiro, D., Stone, B. L., Fassl, B., Nkoy, F., Uchida, D. A., Ward, R. M., Veranth, J. M., and Reilly, C. A. (2016) Characterization of Transient Receptor Potential Vanilloid-1 (TRPV1) Variant Activation by Coal Fly Ash Particles and Associations with Altered Transient Receptor Potential Ankyrin-1 (TRPA1) Expression and Asthma. *J. Biol. Chem. 291*, 24866−24879.
(36) Edgar, R., Domrachev, M., and Lash, A. E. (2002) Gene Expression Omnibus: NCBI gene expression and hybridization array data repository. *Nucleic Acids Res. 30*, 207−210.
(37) Nemmar, A., Subramaniyan, D., and Ali, B. H. (2012) Protective Effect of Curcumin on Pulmonary and Cardiovascular Effects Induced by Repeated Exposure to Diesel Exhaust Particles in Mice. *PLoS One 7*, e39554.
(38) Ma, T., Fukuda, N., Song, Y., Matthay, M. A., and Verkman, A. S. (2000) Lung fluid transport in aquaporin-5 knockout mice. *J. Clin. Invest. 105*, 93−100.
(39) Bevans, T., Deering-Rice, C., Stockmann, C., Light, A., Reilly, C., and Sakata, D. J. (2016) Inhaled Remifentanil in Rodents. *Anesth. Analg. 122*, 1831−1838.
(40) Vogt-Eisele, A. K., Weber, K., Sherkheli, M. A., Vielhaber, G., Panten, J., Gisselmann, G., and Hatt, H. (2007) Monoterpenoid agonists of TRPV3. *Br. J. Pharmacol. 151*, 530−540.
(41) McGarvey, L. P., Butler, C. A., Stokesberry, S., Polley, L., McQuaid, S., Abdullah, H., Ashraf, S., McGahon, M. K., Curtis, T. M., Arron, J., Choy, D., Warke, T. J., Bradding, P., Ennis, M., Zholos, A., Costello, R. W., and Heaney, L. G. (2014) Increased expression of bronchial epithelial transient receptor potential vanilloid 1 channels in patients with severe asthma. *J. Allergy Clin. Immunol. 133*, 704−712.
(42) Li, X., Zhang, Q., Fan, K., Li, B., Li, H., Qi, H., Guo, J., Cao, Y., and Sun, H. (2016) Overexpression of TRPV3 Correlates with Tumor Progression in Non-Small Cell Lung Cancer. *Int. J. Mol. Sci. 17*, 437.
(43) Gorguner, M., and Akgun, M. (2010) Acute Inhalation Injury. *Eurasian J. Med. 42*, 28−35.
(44) Kasurinen, S., Jalava, P. I., Happo, M. S., Sippula, O., Uski, O., Koponen, H., Orasche, J., Zimmermann, R., Jokiniemi, J., and Hirvonen, M.-R. (2017) Particulate emissions from the combustion of birch, beech, and spruce logs cause different cytotoxic responses in A549 cells. *Environ. Toxicol. 32*, 1487−1499.
(45) Bessac, B. F., and Jordt, S. E. (2008) Breathtaking TRP channels: TRPA1 and TRPV1 in airway chemosensation and reflex control. *Physiology 23*, 360−370.
(46) Wu, S.-w., Lindberg, J. E. M., and Peters, J. H. (2016) Genetic and pharmacological evidence for low-abundance TRPV3 expression in primary vagal afferent neurons. *Am. J. Physiol. - Regulatory, Integrative Comparative Physiol. 310*, R794−R805.
(47) Xu, H., Ramsey, I. S., Kotecha, S. A., Moran, M. M., Chong, J. A., Lawson, D., Ge, P., Lilly, J., Silos-Santiago, I., Xie, Y., DiStefano, P. S., Curtis, R., and Clapham, D. E. (2002) TRPV3 is a calcium-permeable temperature-sensitive cation channel. *Nature 418*, 181−186.
(48) Plevkova, J., Kollarik, M., Poliacek, I., Brozmanova, M., Surdenikova, L., Tatar, M., Mori, N., and Canning, B. J. (2013) The role of trigeminal nasal TRPM8-expressing afferent neurons in the antitussive effects of menthol. *J. Appl. Physiol. 115*, 268−274.
(49) Willis, D. N., Liu, B., Ha, M. A., Jordt, S.-E., and Morris, J. B. (2011) Menthol attenuates respiratory irritation responses to multiple cigarette smoke irritants. *FASEB J. 25*, 4434−4444.

DOI: 10.1021/acs.chemrestox.7b00336
Chem. Res. Toxicol. 2018, 31, 291−301